Synthesis, Characterization, and Optical Properties of Metal-Containing Fluorinated Polyimide Films

Takashi Sawada* and Shinji Ando†

NTT Science and Core Technology Laboratory Group, 3-9-11 Midori-cho, Musashino-shi, Tokyo 180-8585, Japan

Five kinds of metal-containing fluorinated polyimide films were prepared by thermal curing of poly(amic acid)s containing metallic salts or organometallic complexes. The chemical states, average sizes, and spatial distribution of the metallic particles were examined, and the thermal and optical properties of the films were compared with those of the colorless host polyimide. For characterizing the metal-containing polyimide films, measurements of refractive indices and wide-angle X-ray diffraction were newly applied. Copper and palladium complexes were fully or partially oxidized to form metal oxide particles, and silver complexes and gold salts were converted into metal particles after thermal imidization. All the films were much less transparent in the visible region than the host polyimide. However, the metal-containing films, except for the gold-containing film, transmitted higher than 80% at 1550 nm near-infrared. The precipitated silver and gold particles increased the average refractive indices of the polyimides.

Introduction

Metal-containing polyimides were first reported by Angelo,[1] who added organometallic complexes to several types of polyimides and reported the metallic contents, dielectric constants, and volume resistivity for the copper-containing polyimides. Polyimide films containing metal/metal oxide particles generated in situ have been studied extensively by Taylor with several collaborative teams in an attempt to synthesize materials with unique electrical, magnetic, thermal, or adhesive properties.[2–12] They have incorporated more than 20 metallic salts and organometallic complexes in aromatic polyimides. Dianhydrides and diamines that have ether (−O−), thioether (−S−), and carbonyl (−CO−) linkages, such as 3,3′,4,4′-benzophenonetetracarboxylic acid dianhydride (BTDA), 4,4′-bis(3,4-dicarboxyphenoxy)diphenyl sulfide (BDSDA), 4,4′-oxydianiline (ODA), and 4,4′-diaminodiphenyl sulfide (DDS) were used. More recently, Rubira et al. reported obtaining highly reflec-

tive silver-containing polyimide films, whose reflectivity was as high as 65%, from the combination of BTDA/ODA and the organosilver complex.[13] This material is attractive for space applications.

Members of our group have reported that fluorinated polyimides derived from 2,2′-bis(trifluoromethyl)-4,4′-diaminobiphenyl (TFDB) exhibit excellent properties needed for optical communication applications.[14] In particular, the polyimide derived from TFDB as a diamine and from pyromellitic dianhydride (PMDA) and/or 2,2-bis(3,4-dicarboxyphenyl)hexafluoro propane dianhydride (6FDA) as dianhydrides, shows high transparency in the visible region (400–800 nm) and low optical transmission losses in the near-infrared region (800–1700 nm), as well as low dielectric constants, low refractive indices, and low water absorption. They demonstrated that single-mode embedded waveguides can be fabricated with these fluorinated polyimides. To fabricate these single-mode waveguides, precise control of the shape and size of the core and of the refractive indices of the core and the cladding was achieved. These waveguides have optical losses of less than 0.3 dB/cm at 1300 nm,[15] and the increase in optical loss was less than 5% in the following two experiments: after heating at 380 °C for 1 h and at 85 °C with a relative humidity of 85% for over 200 h.[16] In these properties, the fluorinated polyimides we developed are superior to those of conventional nonfluorinated polyimides. Nonfluorinated polyimides have a high water absorption of

---

* To whom all the correspondence should be addressed.

† Present address: Tokyo Institute of Technology, Department of Polymer Chemistry, Ookayama 2-12-1, Meguro-ku, Tokyo 152-8553, Japan.

(1) Angelo, R. J. U.S.Patent 3,073,785, 1959.
(2) Taylor, L. T.; Carver, V. C.; Furstch, T. A. *ACS Symp. Ser.* **1980**, *121*, 71.
(3) Furstch, T. A.; Taylor, L. T.; Fritz, T. W.; Fortner, G.; Khor, E. *J. Polym. Sci., Polym. Chem. Eds.*, **1982**, *20*, 1287.
(4) St. Clair, A. K.; Taylor, L. T. *J. Appl. Polym. Sci.*, **1983**, *28*, 2393.
(5) Ezzell, S. A.; Furstch, T. A.; Khor, E.; Taylor, L. T. *J. Polym. Sci., Polym. Chem. Eds.*, **1983**, *21*, 865.
(6) Ezzell, S. A.; Taylor, L. T. *Macromolecules* **1984**, *17*, 1627.
(7) Rancourt, J. D.; Taylor, L. T. *Macromolecules* **1987**, *20*, 790.
(8) Madeleine, D. G.; Spillane, S. A.; Taylor, L. T. *J. Vac. Sci. Technol.* **1987**, *A5*, 347.
(9) Porta, G. M.; Taylor, L. T. *J. Mater. Res.* **1988**, *3*, 211.
(10) Rancourt, J. D.; Porta, G. M.; Taylor, L. T. *Chem. Mater.* **1989**, *1*, 269.
(11) Bergmeister, J. J.; Taylor, L. T. *Chem. Mater.* **1992**, *4*, 729.
(12) Ellison, M. W.; Taylor, L. T. *Chem. Mater.* **1994**, *6*, 990.
(13) Rubira, A. F.; Rancourt, J. D.; Caplan, M. L.; St. Clair, A. K.; Taylor, L. T. *Chem. Mater.* **1994**, *6*, 2351.
(14) Matsuura, T.; Ando, S.; Sasaki, S.; Yamamoto, F. *Macromolecules* **1994**, *27*, 6665.
(15) Matsuura, T.; Ando, S.; Sasaki, S.; Yamamoto, F. *Electron. Lett.* **1993**, *29*, 269.
(16) Matsuura, T.; Ando, S.; Matsui, S.; Sasaki, S.; Yamamoto, F. *Electron. Lett.* **1993**, *29*, 2107.

about 1.3−2.9 wt %.[17] This causes significant optical loss at 1300 and 1550 nm, the wavelengths for optical communication, because water molecules have strong absorption peaks in the near-infrared region.[18]

In this study, we made an attempt to investigate the optical properties of metal-containing fluorinated polyimides as novel thermally stable polymeric materials that have some interesting optical functions in the visible and the near-infrared region. Boggess and Taylor have examined visible transmission spectra and coloration of cobalt-containing poly(amic acid)s (PAA) and polyimides.[19] They reported that the colors observed for the PAA solutions differed because of the yellowish color of the PAA derived from BTDA and the nearly colorless appearance of the PAA derived from BDSDA. With thermal imidization and further curing at 300 °C, the characteristic absorption at 650 nm that originates from the Co^{2+}−solvent complexes disappeared and considerable darkening occurred.

For investigation of the effect of the final curing temperature, polyimides are needed whose optical properties are stable over 300 °C. The fluorinated polyimides developed by members of our group show almost no color and their transmittance and refractive indices are stable even after curing at 380 °C. This polyimide is desirable for the purpose of this study as a matrix polyimide.

Further, nanometer-sized metal particles are known to have interesting optical functions such as characteristic coloration and optical nonlinearity.[20] Prior to describing the specific applications to optical communication use, we report here the thermogravimetric analysis, X-ray diffraction patterns, transmission electron micrographs, and basic optical properties of metal-containing fluorinated polyimides, namely optical transmittance, reflectance, and refractive indices. X-ray diffraction and refractive index measurements were newly applied to characterize the metal-containing polyimide films.

Experimental Section

Materials. A fluorinated polyimide, PMDA/TFDB (Figure 1), synthesized from pyromellitic dianhydride and 2,2′-bis-(trifluoromethyl)-4,4′-diaminobiphenyl, was used in this study. The preparation of poly(amic acid) (PAA), the precursor of the polyimide, and the thermal, mechanical, and chemical properties of this polyimide have been described elsewhere.[21] This polyimide exhibits a high polymer decomposition temperature (610 °C), high glass transition temperature (>400 °C), low water absorption (0.7 wt %), and high optical transparency. Five kinds of metallic dopants were used. Bis(2,4-pentanedionato)palladium(II) (Pd(acac)₂) was obtained from Merck, Inc. All the other dopants—tris(2,4-pentanedionato)aluminum(III), (Al(acac)₃), bis(1,1,1-trifluoro-2,4-pentanedionato)copper(II) (Cu-(tfaa)₂), 2,4-pentanedionatosilver(I) (Ag(acac)), and hydrogen tetrachloroaurate(III)trihydrate (HAuCl₄)—were obtained from
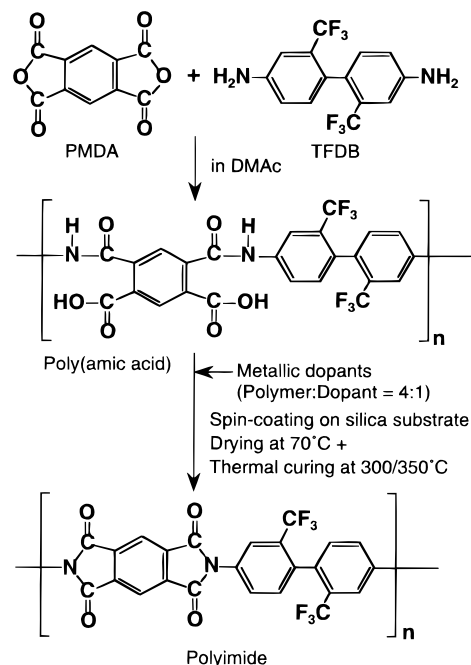

Figure 1. Chemical structures of monomers and preparation of poly(amic acid) and polyimide.

Aldrich Chemical Co. and were used as received. The metal contents of the dopants (with their appearance) are 8.3 wt % for Al(acac)₃ (white), 17.2 wt % for Cu(tfaa)₂ (purple), 34.2 wt % for Pd(acac)₂ (yellow), 52.1 wt % for Ag(acac) (dark brown), and 50 wt % for HAuCl₄ (orange).

Poly(amic acid) Solutions and Film Preparation. Because Al(acac)₃, Cu(tfaa)₂, and HAuCl₄ showed good solubility in the *N,N*-dimethylacetamide (DMAc) solution of PAA (10 wt %), they were added as solids to the solutions. The metallic dopants of low solubility, Pd(acac)₂ and Ag(acac), were added to the PAA solutions with several drops of hexafluroacetylacetone (HFAA). This technique was reported by Caplan et al., who found that a small portion of HFAA considerably improves the solubility of metallic dopants.[23] Addition of metallic dopants into the PAAs was in a 1:4 mol ratio. All the synthesis and mixing procedures were performed in a nitrogen atmosphere. A glovebox was used because the source materials of PAA and some of the dopants are deliquescent or moisture-sensitive. The solutions were stirred for more than 12 h at room temperature and spin-coated onto a fused silica substrate (thickness, 2.5 mm). Both surfaces of the substrate were ground to optical flatness (sureface roughness, ±10 nm) in order to measure the transmittance and refractive indices of the polyimide films without peeling them from the substrates. As a substrate material for the optical measurements, fused-silica is superior to silicon wafers and soda-lime glass because of its high transparency at short wavelengths in the visible region and low refractive index in the visible and near-infrared region.

Polyimide Film Preparation. The PAA solutions with and without metallic dopants on substrates were dried in nitrogen at 70 °C for 1 h and then thermally imidized by heating at a rate of 4 °C/min in a nitrogen atmosphere 15 L/min to the final curing temperature. Polyimides were kept at the final curing temperature for 1 h and then cooled to room temperature. Two series of films with different final curing temperatures (300 and 350 °C) were prepared in this study because significant dopant decomposition or crystal growth occurred in this temperature range.

Measurements. *Vis-NIR Spectrum*. The transmission and reflectance spectra in the visible and near-infrared region (Vis-NIR, $\lambda = 200-2000$ nm) of the polyimide films on substrates

(17) Product Bulletin H-1A, E. I. du Pont de Nemours and Company.

(18) Ando, S.; Matsuura, T.; Sasaki, S. *ACS Symp. Ser.* **1993**, *537*, 304.

(19) Boggess, R. K.; Taylor, L. T. *J. Polym. Sci., Polym. Chem. Ed.* **1987**, *25*, 685.

(20) *Nonlinear Optics of Organics and Semiconductors;* Kobayashi, T., Ed.; Springer-Verlag: Berlin, 1989; Part II.

(21) Matsuura, T.; Hasuda, Y.; Nishi, S.; Yamada, Y. *Macromolecules* **1991**, *24*, 5001.

(22) Matsuura, T.; Yamada, N.; Nishi, S.; Hasuda, N. *Macromolecules* **1993**, *26*, 419.

(23) Caplan, M. L., Southward, R. E., Thompson, D. W.; St. Clair, A. K. *Polym. Mater. Sci. Eng., Am. Chem. Soc.* **1994**, *71*, 787.

were measured using a Hitachi U-3500 spectrophotometer. The reflectance spectra were obtained with a 5° specular reflectance attachment. The same silica substrate, which has >99% transmittance between 200 and 2000 nm, was used as a reference in the transmission measurement, and an SiO_2-coated aluminum mirror was used as a 100%-reflectivity standard in the reflectance measurement. The reflectance spectra in the ultraviolet region (200−400 nm) are not sufficiently accurate, because the reflectivity of the standard mirror is less than 90%.

Refractive Index Measurement. Because polyimides are known as optically anisotropic materials, refractive indices should be measured in the two polarization directions, parallel (n_{TE}, refractive index of transverse electric wave) and perpendicular (n_{TM}, refractive index of transverse magnetic wave) to the film plane.[24,25] A near-infrared wavelength of 1523 nm was used to preclude the influence of absorption. This wavelength is located in the valley between the absorption peaks, which is called a *window.* The prism coupling method[26] was adopted to prevent overestimation of the refractive index near the film surface. This technique can estimate the n_{TE} and n_{TM} averaged over film thickness because it measures the propagation condition of the polarized light inside the films. The refractive indices for the host and metal-containing polyimides were measured using a Metricon PC-2000 refractometer. A helium−neon gas laser (Meres-Griot 05-LIP-171) was used as a light source.

Thermal Gravimetric Analysis. Thermogravimetric analysis (TGA) was conducted on small amounts (about 10 mg) of metallic dopants and metal-containing polyimide films peeled from the substrates using a Shimadzu TGA-50 analyzer. Dopants and polyimide films were heated to 900 °C at 10 °C/min under nitrogen. The polymer decomposition temperature (PDT) was determined as the point of 10% weight loss.

Wide-Angle X-ray Diffraction. Wide-angle X-ray diffraction (XRD) patterns were obtained with a two-axis X-ray diffractometer (Rotaflex RU-300) for the polyimide films together with silica substrates. Cu Kα radiation monochromatized by a silicon crystal scattered from the samples was detected by a scintillation counter through two receiving slits. The average sizes of the metallic crystallites (D) in polyimide films were calculated using Scherrer's formula:[27]

$$D = \frac{0.9\lambda}{\beta \cos \theta} \tag{1}$$

where λ is the wavelength of the X-ray, and β and θ are the half-width and the Bragg angle of the diffraction peaks, respectively. The largest diffraction peaks in the XRD patterns were used for estimating the size of the crystallites. It should be noted that this method can estimate only the average size of the crystallites, not of the particles. This method cannot determine the size of the particles when a metallic particle consists of polycrystallites.

Transmission Electron Micrograph. Cross-sectional transmission electron micrographs of the metal-containing polyimides, except for the aluminum-containing films, were taken with a Hitachi H-8000 transmission electron microscope. The polyimides cured at 300 °C were peeled from the substrates, embedded in epoxy resin, and then sectioned into 50−100 nm thicknesses with a Reichert-Jung Werke ultramicrotome (Ultracut-N).

Results and Discussion

Thermal Decomposition of Dopants. Figure 2 shows the thermal gravimetric profiles of the metallic

(24) Russel, T. P.; Gugger, H.; Swalen, J. D. *J. Polym. Sci., Polym. Phys. Ed.* **1983**, *21*, 1745.

(25) Ando, S.; Sawada, T.; Inoue, Y. *ACS Symp. Ser.* **1994**, *579*, 283.

(26) Tien, P. K.; Ulrich, R.; Martin, R. J. *Appl. Phys. Lett.* **1969**, 14, 291.

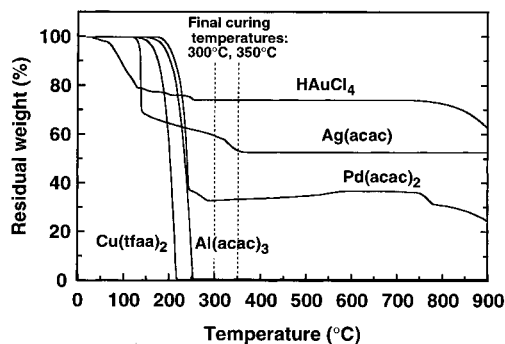(27) Scherrer, P. *Göttingen Nacher.* **1918**, 98.

Figure 2. Thermogravimetric profiles of the metallic dopants tested in nitrogen.

dopants. The weights of all the compounds began to decrease below 200 °C and were almost constant at 350 °C (the higher final curing temperature) with the following exceptions. $Al(acac)_3$ and $Cu(tfaa)_2$ were completely evaporated at 255 and 219 °C, respectively. These temperatures were much lower than the final curing temperature of the polyimides. In the curious profile of $Pd(acac)_2$, the residual weight at 280−300 °C (33%) was close to the Pd content (34.9%); however, complex reactions containing disproportionation are suggested from the gradual increase of weight over 300 °C. The residual weight of Ag(acac) over 360 °C (52%) was equal to that of the metal contents (52.1%), indicating that this dopant was reduced to zerovalent silver (Ag) by thermal treatment. The weight decrease of $HAuCl_4$ below 120 °C was caused by the evaporation of the crystal water and the decomposition of $HAuCl_4$ to $AuCl_3$, because the residual weight between 260 and 750 °C (75%) was close to the weight of $AuCl_3$ (77%). Subsequent decomposition began at 750 °C and did not terminate at 900 °C. This indicates that $HAuCl_4$ was not reduced to zerovalent gold (Au) by thermal treatment below 900 °C. Although these evaporation and decomposition reactions are not necessarily reproduced in the polyimide films, one can expect that decomposition of metallic dopants and subsequent chemical reactions will occur below 350 °C.

XRD Patterns of Polyimides. Table 1 shows the appearance, strength, and PDTs of the host and the metal-containing fluorinated polyimide films cured at 300 °C. The host polyimide without metallic dopants is denoted as FPI, and other polyimides are denoted by the capitalized symbols for the metals containing them. The numbers in the sample abbreviations indicate the final curing temperature. Parts a−f of Figure 3 show the XRD patterns of the polyimide films cured at 300 and 350 °C. When metallic dopants are decomposed by thermal curing and the resultant compounds are crystallized in the polyimide films, characteristic patterns specific to the crystallites of the respective metals or metallic compounds should be observable. The FPI and AL films gave featureless profiles that originated from the amorphous nature of the polyimides and the silica substrate (Figure 3a,b). In addition, there was no difference between the 300 and the 350 °C profiles for these films. From these patterns, one cannot obtain evidence that metallic compounds remain in the aluminum-doped polyimides. However, their appearance, thermal resistance, and optical properties were considerably different from those of the host polyimide, as

Table 1. Host and Metal-Containing Fluorinated Polyimides Cured at 300 °C

polymer	abbreviation	appearance		strength	PDT (°C)[a]
		atmosphere side	substrate side		
polyimide alone	FPI-300	very pale yellow	very pale yellow	tough, flexible	596
polyimide + Al(acac)$_3$	AL-300	dark yellow	dark yellow	tough, flexible	436
polyimide + Cu(tfaa)$_2$	CU-300	dark brown	dark brown	flexible	406
polyimide + Pd(acac)$_2$	PD-300	dark brown	dark brown[b]	fragile	344
polyimide + Ag(acac)	AG-300	red-brown[b]	red-brown	fragile	505
polyimide + HAuCl$_4$	AU-300	dark purple	khaki	fragile	560

[a] Polymer decomposition temperature (PDT) that corresponds to a 10% weight loss. [b] A lustrous metallic surface appeared after the 350 °C curing.
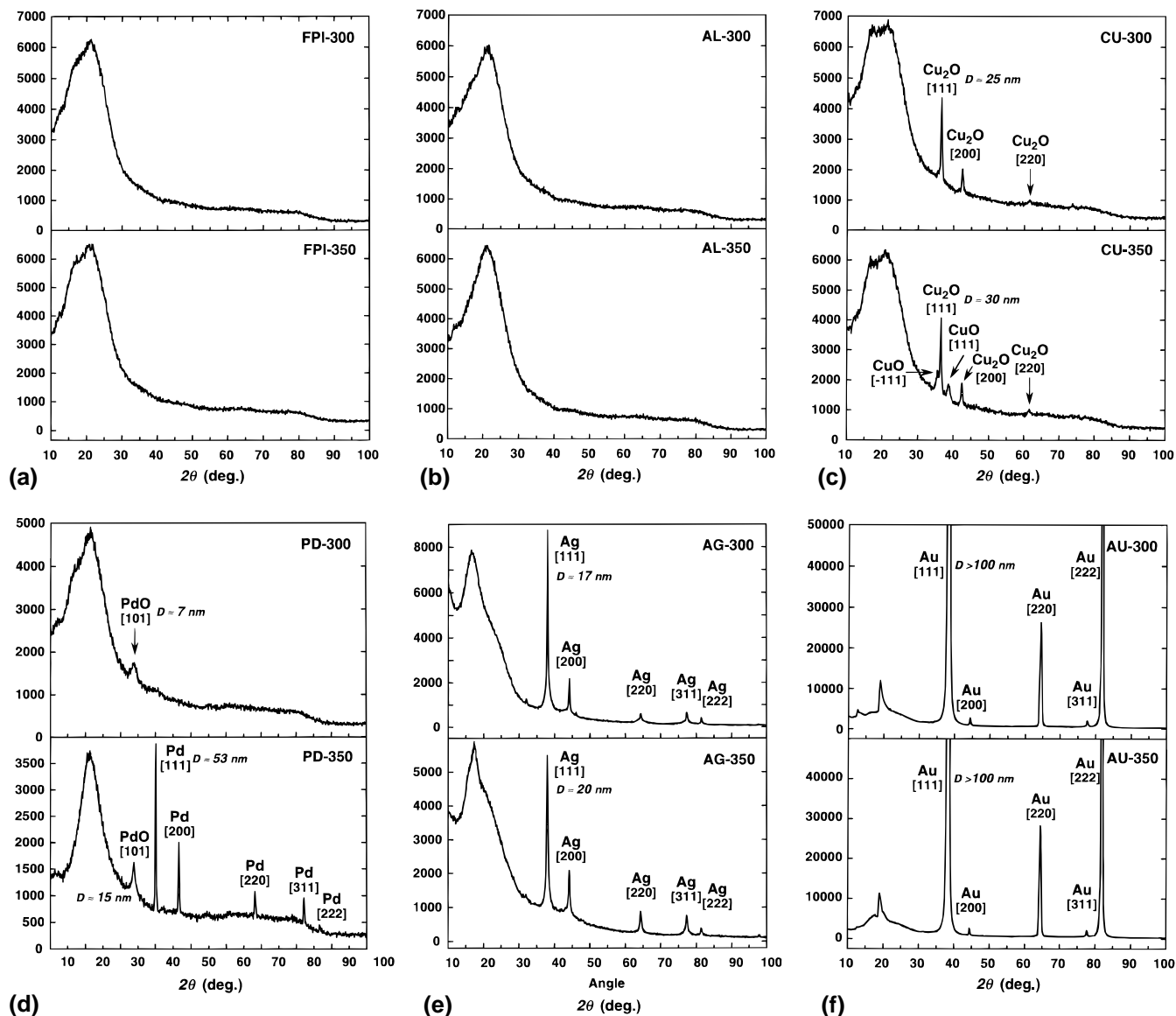

Figure 3. Wide-angle x-ray diffraction patterns of the polyimides cured at 300 °C (top) and 350 °C (bottom): (a) host polyimide (nondoped), (b) aluminum-containing, (c) copper-containing, (d) palladium-containing, (e) silver-containing, and (f) gold-containing polyimides. Average sizes of the precipitated crystallites are inserted (see the text).

described below. The XRD patterns of all the other films, CU, PD, AG, and AU, showed distinct peaks that can be directly ascribed to the respective metals and/or metallic oxides.

In Figure 3c, the CU-300 shows several peaks that can be assigned to copper(I) oxide (Cu$_2$O). This indicates that a reductive atmosphere was generated in the polyimide films during curing. In comparison, two peaks with relatively large half-widths, which are characteristic of copper(II) oxide (CuO), appear in the

CU-350 pattern. This indicates that a portion of the Cu$^+$ ions was oxidized to Cu^{2+} again under the high-temperature curing at 350 °C. In addition, the promotion of the coagulation and crystal growth of Cu$_2$O was evidenced by the decrease in the half-width of the Cu$_2$O [111] peak in the CU-350 pattern. The average size of the newly observed CuO crystals (10 nm) was much smaller than that of the Cu$_2$O crystal (50 nm). In Figure 3d, the PD-300 pattern shows only one broad peak, which can be assigned to palladium(II) oxide

(PdO). Contrary to the CU case, a reductive atmosphere was not dominant under the 300 °C curing, because Pd-(acac)$_2$ and PdO have the same oxidation number, +2. The relatively small average size of the PdO crystal (7 nm) and the absence of peaks of zerovalent palladium (Pd) indicate that the palladium-containing dopant was less reactive in polyimides than the other dopants. However, drastic changes occurred in the XRD pattern and in the appearance of this film after the 350 °C curing. A mirrorlike silvery surface formed on the substrate side of this film, which could be seen through the transparent silica substrate. It is interesting to note that this reflective surface was generated at the interface between the silica surface and the polyimide. After this film was peeled from the substrates, a transparent red layer remained on the substrate. This color is characteristic of the plasmon absorption of nanometer-sized palladium particles. In comparison, the atmosphere side of the film exposed to the dynamic nitrogen flux during curing showed a dark brown color without luster. In the XRD pattern of PD-350, five distinct and very sharp new peaks assigned to Pd were observed, indicating that significant reduction occurred between 300 and 350 °C. The average size of the resultant Pd crystallites was relatively large (30 nm). This fact indicates that the Pd particles aggregated and crystallized very efficiently at the substrate-side surface in this temperature range. In contrast with the patterns described above, Figure 3e,f clearly shows that silver- and gold-containing dopants are easily reduced to the zerovalent metal and are crystallized in the polyimide films by 300 °C curing. The 350 °C curing caused faintly reflective metallic surface to appear on the atmosphere-side surface of AG-350, but no reflective surface formed on the substrate side. On the other hand, the reduction of HAuCl$_4$ proceeded more efficiently than the AG case because the diffraction peaks from gold (Au) in Figure 3f are much stronger than the polyimide and substrate peaks. The average size of the Au crystallites is quite large (>100 nm) and cannot be estimated using Scherrer's formula. The surface appearance of AU films is not reflective; the substrate side showed a frosted khaki color. The dark purple color of the atmosphere side is characteristic of the plasmon absorption of nanometer-sized gold particles. There was no distinct change in the XRD patterns of the AG and AU films between 300 °C and 350 °C, with the exception of a slight growth of the crystallites. This behavior in XRD pattern also indicates that silver- and gold-containing dopants are easily reduced to the metal state and that this state is very stable in polyimide films. In addition, it is worth noting that the diffraction peaks from [111] and [222] of Au in the AU-300 and AU-350 patterns had much larger intensities than those of other peaks, compared with standard data for Au crystallites. The intensity ratio of [111] to [200] in Figure 3f was more than 10, while that in the literature is about 1.2.[28] Such discrepancies are not observed in the other films. This intensity ratio difference indicates that the gold crystallites grew anisotropically in the polyimide films and that the [111] lattice plane was preferentially formed
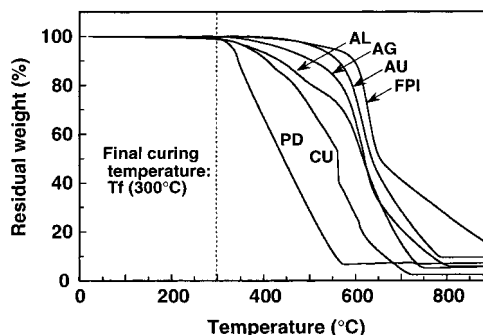
(28) King, M.; MacClune, W. F.; Clark, H. E.; Frank, B. L.; Karmer, T. M.; Zwell, L.; Bernstein, L. R.; Mayo, W. S.; McMurdie, H. F.; Rotella, F. J.; Mrose; M. E. *Powder Diffraction File Computer Database*; JCPDS-International Centre for Diffraction Data: PA, **1996**.

Figure 4. Thermogravimetric profiles of the host and metal-containing polyimides cured at 300 °C.

during curing. Although the XRD patterns have not been used for the analysis of metal-containing polyimide films, we clarified that this method is a powerful tool for identifying the chemical state and crystallite sizes of metallic particles appearing in polyimide films.

Thermal Decomposition of Polyimides. Figure 4 shows the thermal gravimetric profiles of the host and the metal-containing fluorinated polyimides cured at 300 °C. Their PDTs are listed in Table 1. The thermal stabilities of all the metal-containing films were inferior to that of the host polyimide. Boggess and Taylor have pointed out that the presence of metallic compounds serves to catalyze the oxidative degradation of the polyimide films.[19] In particular, PD-300 showed a much lower PDT than other films 250 °C lower than that of host polyimide. The XRD profiles revealed that the reduction became vigorous above 300 °C and thus Pd particles appeared on the substrate side. CU-300 also showed a lower PDT next to PD, where the XRD patterns revealed that the oxidation reaction proceeded over 300 °C. These considerable decreases in PDTs may be related to polymer decomposition related to the oxidation of Cu$_2$O to CuO in the CU film and the reduction of PdO to Pd in the PD film: two other films containing only metal particles (AG and AU) show higher PDTs although still lower than the host polyimide. The TGA curves of AG-300 and AU-300 are similar to that of the host polyimide. These facts indicate that most of the chemical reactions in the films were completed by the 300 °C curing and no significant reaction (except for polymer-chain degradation) occurs above 300 °C. It is noteworthy that AU-300 showed the highest PDT despite its strong XRD peaks and precipitated large particles. From its appearance, the PDT, and the shape of its TGA curve, AL-300 is inferred to contain some metallic compounds. The significant weight decrease between 400 and 450 °C of this film should be related to polymer degradation caused by some reaction of aluminum compounds. The metal-free FPI-300 film showed no weight decrease in this temperature range.

Transmission and Reflectance Spectra. The optical transparency and reflectivity of poly(amic acid) and polyimide films are affected considerably by the incorporation of metallic dopants. Parts a−f of Figure 5 show the Vis-NIR transmission and reflectance spectra of the host and metal-containing PAAs and the polyimides cured at 300 and 350 °C. The FPI-, AL-, and PD-PAA samples were almost colorless. In contrast, the transmission spectra of CU- and AG-PAAs showed
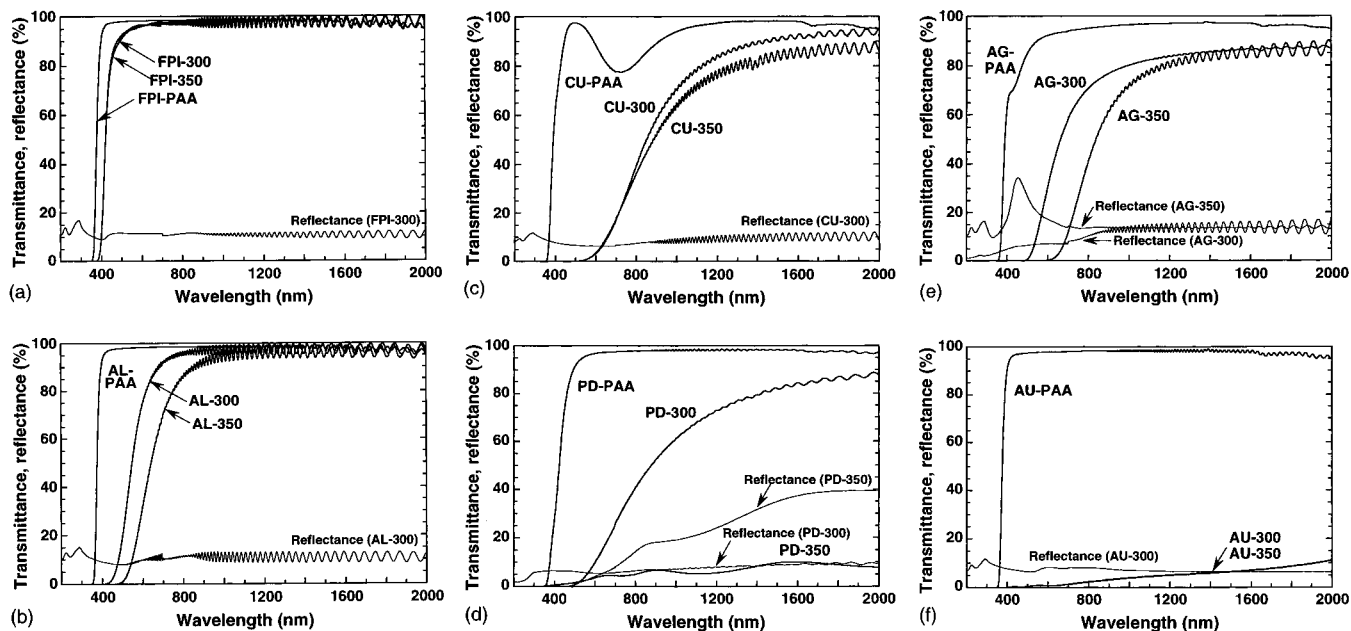
Figure 5. Vis-NIR transmission and reflectance spectra of the polyimides cured at 300 and 350 °C: (a) host polyimide (nondoped), (b) aluminum-containing, (c) copper-containing, (d) palladium-containing, (e) silver-containing, and (f) gold-containing polyimides. The reflectance spectrum of the substrate side of PD-350 (cured at 350 °C) and that of the atmosphere side of AG-350 (cured at 350 °C) are inserted in parts d and e, respectively.

conspicuous colorations, reflecting the deep colors of the dopants. CU-PAA and AG-PAA were clear blue-green and light matte brown, respectively. The former color may originate from the characteristic absorption of the complexes consisting of Cu^{2+} ion and solvent (DMAc). As seen in Figure 5a, the imidization reaction and curing at 300 °C induced a pale yellow color in the polyimide film, but the high-temperature curing at 350 °C caused little change in the transmission spectra. The wavelength of absorption edge (λ_0) of FPI-350 (400 nm) is shorter than those of conventional polyimides ($\lambda_0 = 450$ nm for PMDA/ODA), indicating the high transparency in the visible region of this host polyimide. St. Clair et al. have clarified that the coloration of polyimides is consistent with the intra- and intermolecular charge transfer (CT) interaction.[29,30] Ando et al. have recently discussed the relationships between the color intensities of polyimide films and the electronic properties of their source materials that derived from NMR chemical shifts and molecular orbital calculation.[31] The light color of this polyimide can be explained from the low-electron-donating property of the fluorinated diamine and decreased CT interactions caused by the bulky CF_3 groups that are effective in preventing the CT interaction between polymer chains through steric hindrance. Reflectance of about 10% in the entire range was caused by Fresnel reflection, originating from the difference in refractive indices between air and the polyimide surface.[32] For the aluminum-containing films (Figure 5b), thermal imidization caused significant coloration, and the curing at 350 °C considerably

decreased the transmittance in the visible region, with an accompanying longer wavelength shift of λ_0. The difference in the spectra between 300 and 350 °C was larger than that for CU films. This fact also supports the existence of amorphous metallic compounds[19] in the AL-300 and AL-350 films. The CU-300, PD-300, and AG-300 films showed similar transmission spectra, in which λ_0s were displaced to 550−600 nm by the incorporation of metallic dopants and the transmittance gradually increased with an increase in wavelength. These spectra show the typical shape that was observed for the composite films containing nanoscopic gold particles.[33] Although these films showed considerable coloration and the transparency in the visible region was low (about 40% at 800 nm), the transparency in the near-infrared region was relatively high (more than 80% at 1550 nm) and was within the useful range for optical applications. The transmission spectra of CU-300 and CU-350 did not show a significant change in λ_0, reflecting the slight change in XRD patterns (Figure 5c). A drastic change can be seen in the spectra between PD-300 and PD-350, in which the transmittance was reduced from 80% to less than 15% at 1550 nm by curing at a 50 °C higher temperature (Figure 5d). This difference can be easily observed from their appearance and XRD patterns. As described above, a mirrorlike surface was formed at the interface between the silica and the polyimide of PD-350, and very intense XRD peaks assigned to Pd appeared. When the film was peeled from the substrate, the colored layer remained in the film. The reflectance spectrum of this surface (substrate side of the peeled film) is incorporated in Figure 5d, showing the high reflectance of around 30−40% in the NIR region. The reflectance spectra of the atmosphere side of the AL-300, CU-300, and PD-300

(29) St. Clair, A. K.; St. Clair, T. I. *Am Chem. Soc. Div. Polym. Mater. Sci. Eng.* **1984**, 51, 62.
(30) St. Clair, A. K.; St. Clair, T. I.; Slemp, W. S.; Ezzell. K. S. *Proceedings of the 2nd Ηuternational Conference on Polyimides*; Ellenville, NY, 1985; p 333.
(31) Ando, S.; Matsuura, T.; Sasaki, S. *Polymer J.* **1997**, *29*, 69.
(32) Born, M.; Wolf, E. *Principles of Optics*, 5th ed.; Pergamon Press: Oxford, 1975; Chapter 1.

(33) Foss, C. A.; Hornyak, G. L.; Stokert, J. A.; Martin, C. R. *J. Phys. Chem.* **1992**, *96*, 7497.

Table 2. Refractive Indices and Birefringence of Host and Metal-Containing Fluorinated Polyimides

polyimides	n_{TE}[a]	n_{TM}[a]	n_{ave}	Δn
FPI-300	1.6060	1.4892	1.5671	0.1168
AL-300	1.6022	1.5001	1.5682	0.1021
CU-300	1.6059	1.5045	1.5721	0.1014
PD-300	1.6037	1.5035	1.5703	0.1002
AG-300	1.6237	1.5014	1.5829	0.1223
AU-300	1.6356	1.5034	1.5915	0.1322

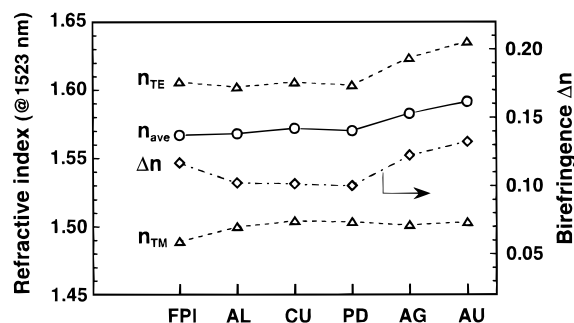[a] Measured at 1523 nm using a prism coupling method.

Figure 6. Refractive indices parallel (n_{TE}) and perpendicular (n_{TM}) to the film plane, average refractive indices (n_{ave}), and in-plane/out-of-plane birefringences (Δn) of the host and metal-containing polyimides cured at 300 °C.

films were the same as that of the host polyimide. Despite the absence of change in the appearance and XRD patterns of AG-300 and AG-350, the transmission spectra of these films showed a significant change in λ_0 (Figure 5e). Another striking feature in this figure is that the atmosphere side of the AG-350 film shows a distinct peak of 35% at 480 nm in the reflectance spectrum. This coincides with the fact that a reflective surface with silvery color formed on the atmosphere side of AG-350. The wavelength of the reflection peak coincided with that of the characteristic plasmon absorption of a metallic silver surface. The presence of a reflection peak and the silvery color indicates that Ag particles concentrated near the atmosphere-side surface. The AU-300 and AU-350 films showed very low transmittance in the Vis-NIR region, but a slight increase in transmittance with increasing wavelength was observed. The large zerovalent gold (Au) particles confirmed in the XRD patterns absorbed and scattered the incident light. As described below, the average size of the Au particles in these films was much larger than that determined from the XRD patterns, indicating that the particles consisted of many crystallites.

Refractive Indices. Refractive indices and their anisotropy (birefringence) of polyimide films are thought to be affected by the incorporation of metallic dopants.[34] Because the n_{TE}s of the films prepared on silica substrates are isotropic in the film plane, the average refractive index (n_{ave}) and the birefringence (Δn) of polyimides can be defined as $(2n_{TE} + n_{TM})/3$ and $(n_{TE} - n_{TM})$, respectively.[14] Table 2 and Figure 6 show the refractive indices and the birefringence measured for the host and the metal-containing polyimides cured at 300 °C. The n_{ave}s of all the metal-containing polyimides were larger than that of the host polyimide (FPI). This

(34) Maxwell–Garnett, J. C. *Philos. Trans. R. Soc., London* **1904**, *203*, 385. Maxwell–Garnett, J. C. *Philos. Trans. R. Soc., London* **1906**, *205*, 237.
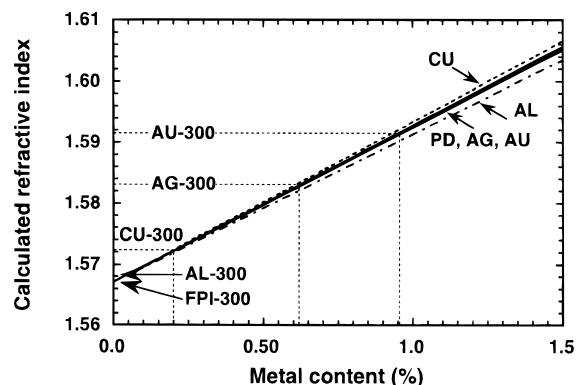

Figure 7. Refractive indices of metal-containing polyimides calculated using the Maxwell–Garnett theory.

result should be related to the generation of metal or metallic particles in polyimide films. From the definition of n_{ave}, the slight increase in n_{ave} of AL, CU, and PD films was caused by the increase in n_{TM}s, because the n_{TE}s were not affected by the incorporation of metallic dopants. No peaks of zerovalent metals were detected in the XRD patterns of these films. On the other hand, the n_{TE}s were more influential in the increase of n_{ave}s in AG and AU films whose the XRD patterns clearly showed the generation of zerovalent metal particles. The Δns of the former films (AL, CU, and PD) were smaller and those of the latter (AG and AU) films were larger than that of FPI for the same reasons as described above.

A theoretical model for estimating the dielectric permittivity (ϵ) of the composite films containing nanoscopic metal particles was set up by Maxwell–Garnett (M–G), using the assumption that the particles are spherical and sufficiently small with respect to the wavelength of incident light.[34] According to the M–G theory, ϵ is related to the dielectric permittivities of the metal (ϵ_m) and the host film (ϵ_0) via

$$\frac{\epsilon - \epsilon_0}{\epsilon + 2\epsilon_0} = f_m \frac{\epsilon_m - \epsilon_0}{\epsilon_m + 2\epsilon_0} \qquad (2)$$

where f_m is the volume fraction occupied by the metal particles. Because the frequency of the alternating electric field is sufficiently high in the Vis-NIR region, the dielectric permittivity can be expressed as the square of the refractive index.

$$\epsilon = n^2 \qquad (3)$$

Assuming that nanometer-sized spherical metal particles are homogeneously dispersed in the polyimide films, the refractive indices of the metal-containing polyimides can be calculated from the refractive indices of metals and host polyimides. Figure 7 shows the calculated refractive indices of the polyimides as a function of the volume fraction of the metal particles. The refractive indices used were 1.44−i 16.0 for aluminum, 0.606−i 8.26 for copper, 2.957−i 8.30 for palladium, 0.469−i 9.32 for silver, 0.559−i 9.81 for gold, and 1.5671 for the host polyimide at 1.55 μm, where i is $(-1)^{1/2}$.[35] The imaginary portion of the calculated

(35) Palik, E. D. *Handbook of Optical Constants of Solids*; Academic Press: New York, 1985.

Table 3. Calculated Weight Fraction, Density, and Calculated Volume Fraction of Metal Particles in Polyimides and Volume Fractions Calculated from Their Refractive Index

polyimides	$f_W{}^a$ (%)	d (g/cm³)	$f_V{}^a$ (%)	$f_{V,\text{ref}}$ (%)
AL-300	1.16	2.69	0.63	0.04
CU-300	2.67	8.93	0.45	0.19
PD-300	4.60	12.2	0.57	0.13
AG-300	4.87	10.5	0.71	0.63
AU-300	8.20	19.3	0.67	0.98

[a] Assuming that all the dopants are deoxidized and precipitated as zerovalence metal particles.

refractive indices was negligibly small (<0.001). The refractive index of metal-containing polyimide increases monotonically as a function of the metal fraction. Although the dependence of the refractive index on the kinds of metal is small, silver and gold particles confirmed to exist in the polyimide films showed the same dependence on the metal fraction. Assuming that all the dopants were reduced to the zerovalent state and precipitated homogeneously in the polyimide films, the volume fraction of the metal particles (f_V) can be calculated as

$$f_V = \frac{f_W/d_m}{(1 - f_W)/d_p + f_W/d_m} \qquad (4)$$

where f_W is the weight fraction of the metal particle which can be calculated from the mol ratio of metal dopants and atomic weight, and d_m and d_p are the densities of the metal and the host polyimide (1.45 g/cm³), respectively. Table 3 lists the calculated volume fractions (f_V) as well as the volume fractions ($f_{V,\text{ref}}$) estimated from the average refractive indices, using Figure 7 under the same assumption. Only the AG-300 and AU-300 films, in which metal particles precipitated, showed larger $f_{V,\text{ref}}$s, whereas the other films showed much smaller $f_{V,\text{ref}}$s than f_Vs. Because the dielectric permittivities of metal oxides (Cu₂O, CuO, and PdO) are smaller than those of metals, the CU-300 and PD-300 films showed smaller values for $f_{V,\text{ref}}$. The cause of the $f_{V,\text{ref}}$ of AU-300 being larger than f_V can be ascribed to the inhomogeneous distribution of the gold particles in the film. In addition, the marked increase in n_{TE}s for the AG-300 and AU-300 films indicates that these metal particles were distributed in such a way that the TE polarization of light (electric field of light E, parallel to the film plane) was influenced more than the TM polarization (E perpendicular to the film plane). Such a condition can be attained when the metal particles are arranged in layers parallel to the film plane. This result coincides with the result of the XRD pattern, which indicated that the [111] plane of gold crystallites was preferentially aligned in the film plane.

Transmission Electron Micrographs (TEM). Figures 8−11 show cross-sectional transmission electron micrographs (TEMs) near the atmosphere side and the substrate side for CU-300, PD-300, AG-300, and AU-300 films. The magnifications of Figures 8 and 11 are ×10 000, and those of Figures 9 and 10 are ×100 000. TEMs with a higher magnification of ×300 000 (not shown) were used to evaluate the particle sizes. These
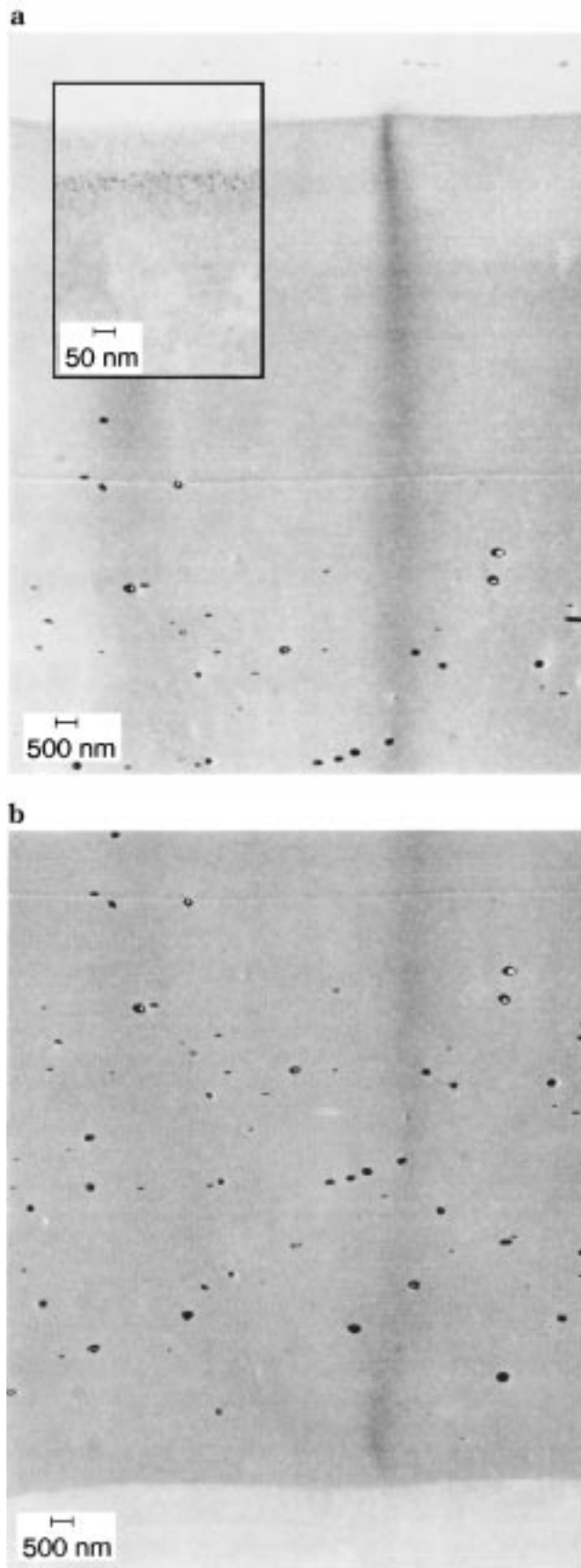

Figure 8. Cross-sectional TEM images of the copper-containing fluorinated polyimide films cured at 300 °C: (a) near the atmosphere side, an image taken with ×100 000 resolution is shown in the insert, and (b) near the substrate side.
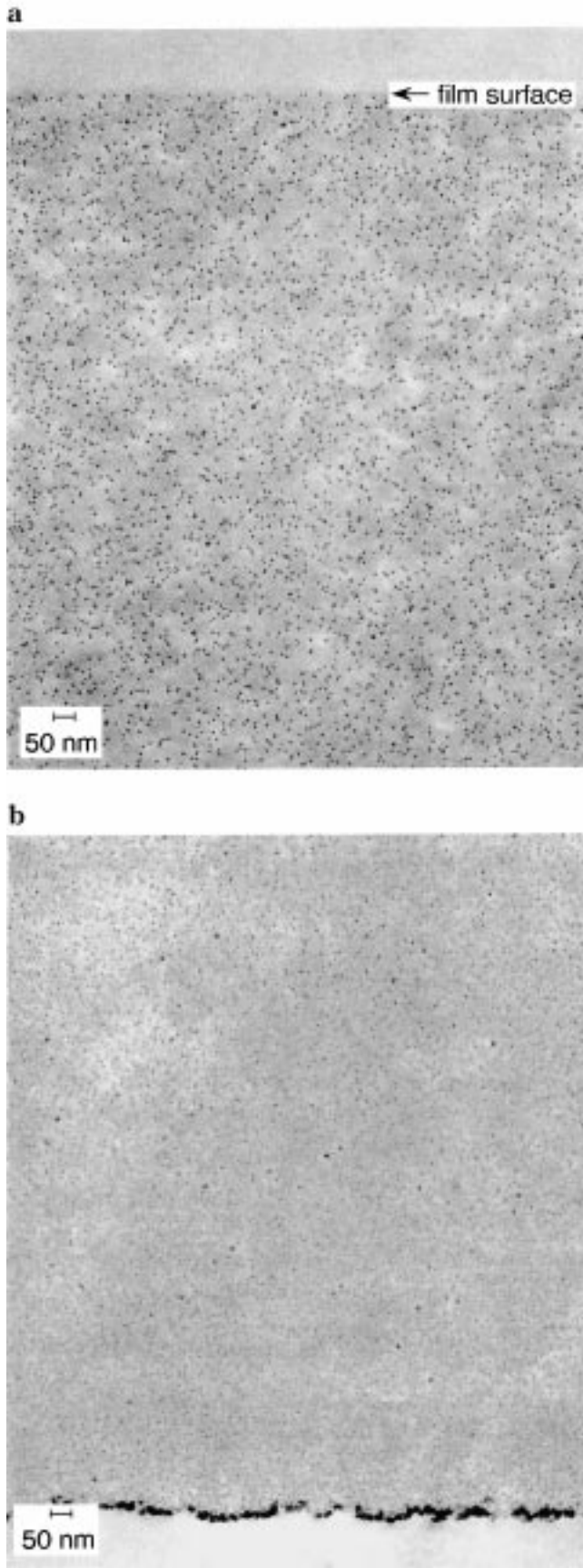
a

b

Figure 9. Cross-sectional TEM images of the palladium-containing fluorinated polyimide films cured at 300 °C: (a) near the atmosphere side and (b) near the substrate side.

a

b

Figure 10. Cross-sectional TEM images of the silver-containing fluorinated polyimide films cured at 300 °C: (a) near the atmosphere side and (b) near the substrate side.

films showed characteristic XRD patterns that can be assigned to metal or metal oxide crystallites. The
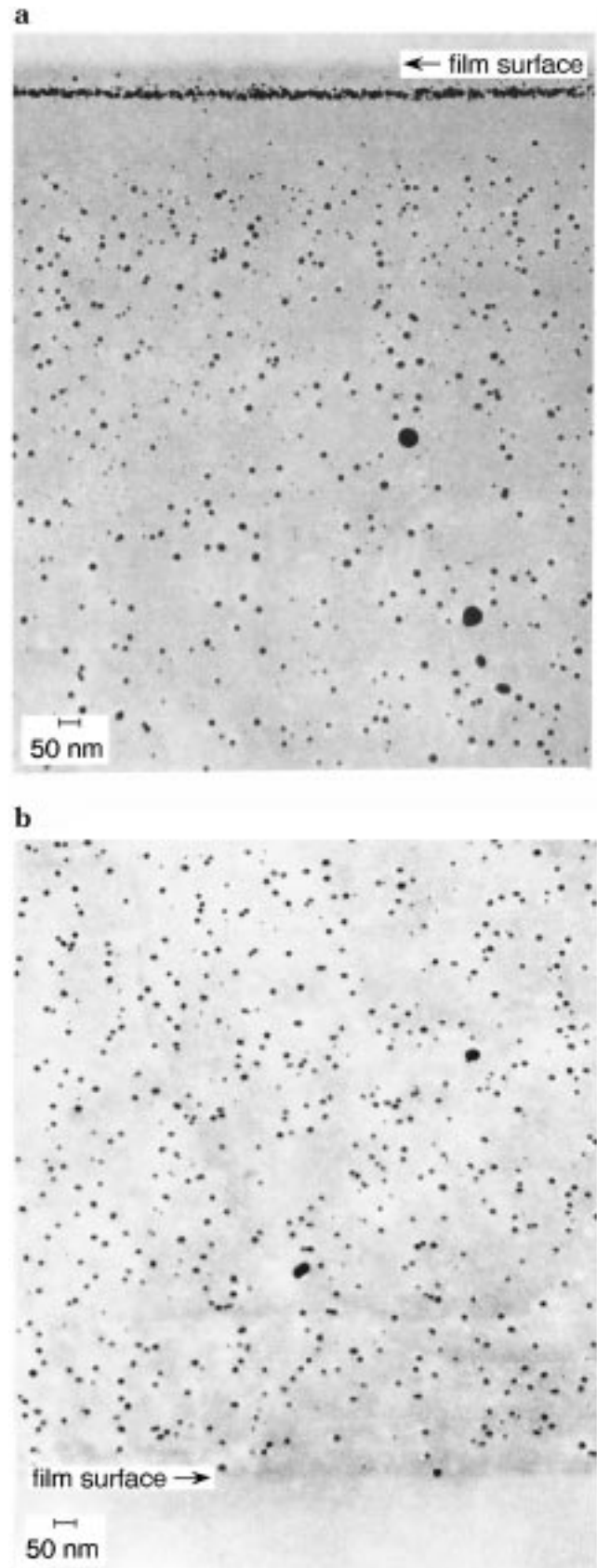
spatial distribution of the precipitated particles shown in the micrographs changed considerably depending on the type of metallic dopants observed.
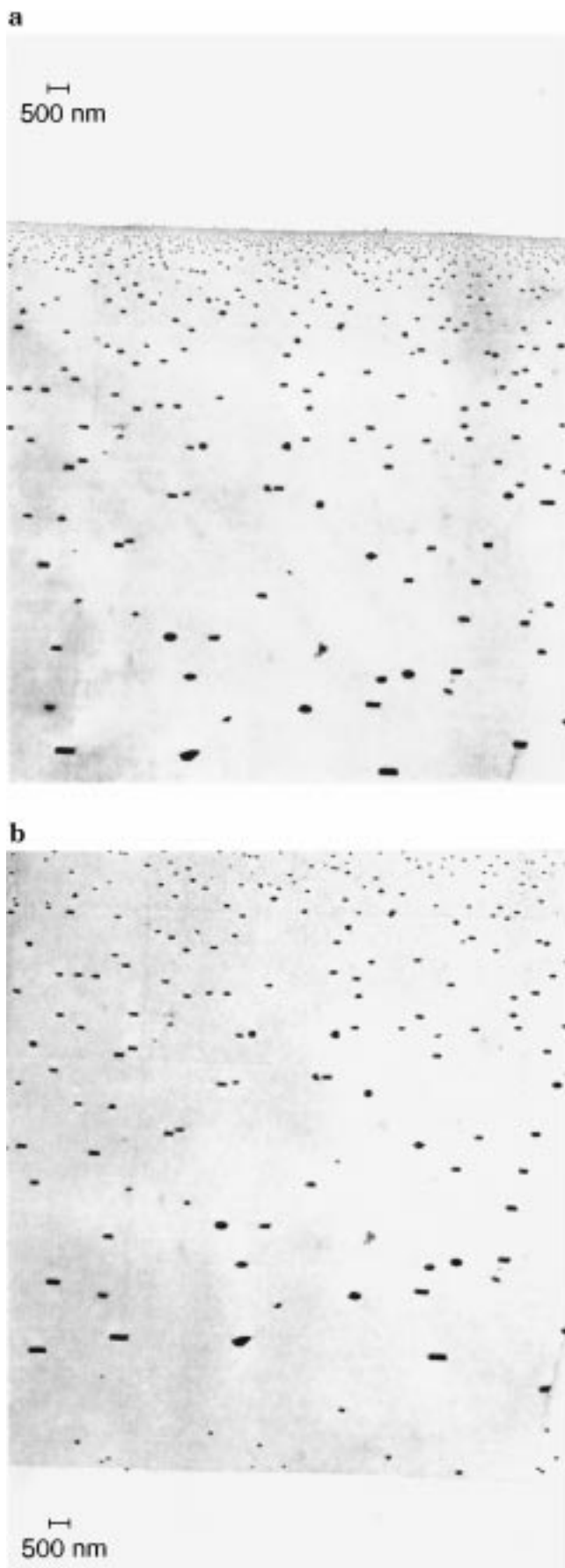
A striking feature in CU-300 is that large metallic particles 50−300 nm in size were found only inside the film, and a 7-μm-thick layer without such particles was present on the atmosphere side (Figure 8a,b). These particles can be identified as aggregates of copper(I) oxide (Cu_2O) crystallites, because the particle sizes in micrographs were several times larger than that of the Cu_2O crystallites determined by XRD (25 nm). However, the TEM of the atmosphere-side region at a resolution of $\times$100 000 shows that a 50-nm-thick layer consisting of nanometer-sized particles resides between the 100-nm-thick polyimide overlayer and the 6−7-μm-thick particle-free layer (see the micrograph incorporated in Figure 8a). Taylor reported that a 5-nm-thick Cu layer was sandwiched between a 6-nm-thick polyimide overlayer and a bulk polyimide near the atmosphere side in a copper-containing polyimide.[9] In the XRD patterns of this study, we did not detect a pattern from Cu crystallites, and the layer containing Cu_2O particles and the polyimide overlayer were about 10 times thicker than those of the reference. The circular white regions surrounded by the metallic particles seen in black in the TEMs are the holes resulting from the removal or the movement of the particles during microtoming.

The metallic particles were uniformly dispersed throughout the film in PD-300, except for the substrate-side surface (Figure 9a,b). The higher magnification micrographs indicate that the particles precipitated near the atmosphere side and the substrate side had a narrow size distribution ranging from 1 to 5 and 1 to 10 nm, respectively. Because the sizes of the dispersed particles were almost equal to those calculated from the XRD pattern (7 nm), these are identifiable as crystallites of palladium(II) oxide (PdO). In addition, a discontinuous layer consisting of the aggregates of particles several tens of nanometers in size, i.e., a densely concentrated layer, resides on the substrate side surface. Miner et al. observed that a densely concentrated metallic layer with a smooth surface was generated on the atmosphere side of a palladium-containing polyimide.[36] This side is opposite to the side observed in this study.

The spatial distribution of the silver particles in AG-300 was similar to that in PD-300; however, a 50-nm-thick, densely concentrated layer appeared 50 nm below the surface, with a thin polyimide overlayer on the atmosphere side. This densely concentrated layer is the cause of the relatively high reflectance of 35% at 480 nm. This silver layer should afford durability against oxidation by air, because the layer is not exposed to the atmosphere. Compared with the sizes of crystallites (17 nm) determined by XRD, the 10−30-nm particles, which were Ag crystallites, uniformly dispersed inside the film. In addition, the densely concentrated layer also consisted of particles of similar sizes. Miner et al. have reported that a densely concentrated layer of silver particles resides on the atmosphere-side surface of the silver-containing polyimide, where the layer consists of much larger particles than the uniformly dispersed particles in the films.[36] The reflectance of the atmosphere-side surface was as much as 60%. The lower reflectance of the atmosphere side surface of the AG-

Figure 11. Cross-sectional TEM images of the gold-containing fluorinated polyimide films cured at 300 °C: (a) near the atmosphere-side and (b) near the substrate side.

(36) Miner, G. A.; St. Clair, A. K.; Stoakley, D. M. *Polym. Mater. Sci. Eng., Am. Chem. Soc.* **1995**, *72*, 355.

350 film can be explained from the fact that the densely concentrated layer was thinner and consisted of much smaller particles.

The Au particles precipitated in AU-300 were distributed uniformly through the film, but the sizes of the particle varied in a very wide range from the atmosphere-side surface to the substrate-side surface. The particles near the atmosphere-side surface (several nm) were about 100 times smaller than those near the substrate-side surface (500 nm). The wide distribution of the sizes of Au particles was also reported by Taylor et al.[8,37] A striking feature of the particles in AU-300 was their anisotropic shapes, with longer parts of 100−500 nm and shorter parts of 50−200 nm. Some of them showed clearly defined rectangular shapes, and they were oriented in the direction parallel to the film plane. This characteristic shape and the orientation of metallic particles were observed only in the gold-containing film. This observation should be closely related to the preferential ordering of the [111] lattice along the film surface, which was observed in the XRD pattern. In addition, the increase in n_{TE} (parallel to the film plane) for AG-300 is explained by the Ag-particle layer near the atmosphere-side surface and that for AU-300 is explained by the anisotropic-shaped Au particles that were oriented parallel to the film surface. In these cases, the metal content seen by the TE-polarized light is larger than that seen by the TM-polarized light, and high metal content always induces the increase in refractive index, as shown in Figure 7.

Conclusion

Five kinds of metal-containing fluorinated polyimide films were prepared by thermal curing of colorless poly-(amic acid)s containing metallic salts or organometallic complexes. Copper and palladium complexes fully or partially oxidized to metal oxide particles, while silver complex and gold salt were converted to metal particles after thermal imidization. All the films, except for the gold-containing film, showed transmittances higher than 80% in the NIR region, and the silver-containing film cured at 350 °C showed a mirrorlike surface with a reflectance higher than 35% at 480 nm. The refractive indices of all films incorporating the metallic dopants were larger than that of the host polyimide. In particular, silver- and gold-containing films in which metal particles precipitated showed larger refractive indices, resulting from their high dielectric permittivities and larger volume fractions of metal particles. The sizes of the metal particles were 1−10 nm for the palladium-containing films, 10−30 nm for the silver-containing film, and several hundred nanometers for the copper- and the gold-containing films. In addition, a concentrated layer of silver particles was found to reside just under the atmosphere surface of the silver-containing polyimide, and a concentrated layer of palladium oxide particles was found at the substrate surface of the palladium-containing film. No metallic particles were observed in the XRD of aluminum-containing film, despite its lower optical transmittance and higher refractive index than those of undoped fluorinated polyimides. It was found that X-ray diffraction measurement is a useful tool for investigating the chemical state, size, and anisotropic growth behavior of the precipitated particles. The refractive index of metal-containing polyimide films also reflects the chemical state and spatial distribution of the precipitated particles. Metal-containing fluorinated polyimides are attractive materials that have high transparency in the near-IR region and interesting optical functionalities originating from the precipitated nanometer-sized metallic particles.

(37) Rancourt, J. D.; Porta, G. M.; Taylor, L. T. *Thin Solid Films* **1998**, *158,* 189.